Available online at www.sciencedirect.com
SCIENCE DIRECT®
Geochimica et Cosmochimica Acta 70 (2006) 640–650
Geochimica
www.elsevier.com/locate/gca

Kinetics of Fe(III) precipitation in aqueous solutions at pH 6.0–9.5 and 25 °C

A. Ninh Pham, Andrew L. Rose, Andrew J. Feitz, T. David Waite *

Centre for Water and Waste Technology, School of Civil and Environmental Engineering, The University of New South Wales, Sydney, NSW 2052, Australia

Received 11 April 2005; accepted in revised form 17 October 2005

Abstract

The kinetics of Fe(III) precipitation in synthetic buffered waters have been investigated over the pH range 6.0–9.5 using a combination of visible spectrophotometry, ^{55}Fe radiometry combined with ion-pair solvent extraction of chelated iron and numerical modeling. The rate of precipitation, which is first order with respect to both dissolved and total inorganic ferric species, varies by nearly two orders of magnitude with a maximum rate constant of $16 \pm 1.5 \times 10^6$ M^{-1} s^{-1} at a pH of around 8.0. Our results support the existence of the dissolved neutral species, $Fe(OH)_3^0$, and suggest that it is the dominant precursor in Fe(III) polymerization and subsequent precipitation at circumneutral pH. The intrinsic rate constant of precipitation of $Fe(OH)_3^0$ was calculated to be $k_{Fe(OH)_3^0} = 2.0 \times 10^7$ M^{-1} s^{-1} allowing us to predict rates of Fe(III) precipitation in the pH range 6.0–9.5. The value of this rate constant, and the variation in the precipitation rate constant over the pH range considered, are consistent with a mechanism in which the kinetics of iron precipitation are controlled by rates of water exchange in dissolved iron hydrolysis species.

1. Introduction

The dynamic behavior of iron in natural waters and its numerous critical roles in living organisms has brought it to the forefront of water chemistry research in the last few decades. The fascinating chemistry and biological impacts of iron arise from its unusual dynamic (non-equilibrium) behavior, which subsequently influences its biological availability. This behavior includes complexation (chelation) of iron by natural organic ligands, redox reactions of various iron species and their complexes via photochemical and/or biological processes, adsorption of ferric and ferrous iron on particle surfaces, and hydrolysis and subsequent precipitation of Fe(III) (Sunda and Huntsman, 2003). Despite its abundance (as the fourth most abundant element in the Earth's crust), iron is present at extremely low concentrations in most natural waters due to the low solubility of the thermodynamically stable oxidation state, Fe(III).

The inorganic chemistry of Fe(III) in natural waters is controlled primarily by its hydrolysis and subsequent precipitation (Waite, 2001). In natural waters, Fe(III) readily hydrolyzes and precipitates, a process that is initiated by the formation of small polymers. These small polymers grow to larger polymers and eventually to colloidal sized hydroxide solids. Despite the importance of these processes, there have been a limited number of investigations of the kinetics of Fe(III) precipitation, although considerable work has been undertaken to investigate the thermodynamic properties and solubility of the particulate iron oxide products over the last few decades (Baes and Mesmer, 1976; Byrne and Kester, 1976a,b; Zafiriou and True, 1980; Flynn, 1984; Kuma et al., 1992; Millero et al., 1995; Kuma et al., 1996; Millero, 1998; Liu and Millero, 1999; Byrne et al., 2000; Byrne and Luo, 2000; Liu and Millero, 2002; Sunda and Huntsman, 2003; Perera and Hefter, 2003). Recently, a study in our laboratory (Rose and Waite, 2003) showed that Fe(III) precipitation in seawater at pH 8.1 was a second order process depending on both

* Corresponding author. Fax: +61 2 93856139.
E-mail address: d.waite@unsw.edu.au (T.D. Waite).

0016-7037/$ - see front matter © 2005 Elsevier Inc. All rights reserved.
doi:10.1016/j.gca.2005.10.018

the dissolved inorganic Fe(III) and total inorganic Fe(III) concentrations, with an apparent rate constant of $4.1 \times 10^7\ M^{-1}\ s^{-1}$. A previous study by Grundl and Delwiche (1993) found that the kinetics of precipitation at low pH is described by an initial slow nucleation rate followed by a more rapid rate of crystallite growth. Both rates were first order in the calculated concentration of aqueous $Fe(OH)_{3(aq)}^0$, and precipitation of the ferric solid from $Fe(OH)_{3(aq)}^0$ was found to be the rate controlling step. This is consistent with the conclusion by Liu and Millero (1999) that the solubility of Fe(III) at pH around 8.0 is apparently determined by $Fe(OH)_{3(aq)}^0$. Our previous study (Rose and Waite, 2003) also supports a mechanism by which $Fe(OH)_{3(aq)}^0$ is the dominant precursor for polymerization in the precipitation process around this pH.

Although many studies have investigated iron hydrolysis behavior, there is still no consensus either on the solubility of Fe(III) or the exact composition of various ferric hydrolysis species (Fe^{3+}, $Fe(OH)^{2+}$, $Fe(OH)_2^+$, $Fe(OH)_{3(aq)}^0$ and $Fe(OH)_4^-$). In particular, the existence of the dissolved $Fe(OH)_{3(aq)}^0$ species is not universally accepted. Byrne and Kester (1976a) reported the presence of $Fe(OH)_{3(aq)}^0$ as the dominant hydrolysis species at circumneutral pH while Hudson et al. (1992) and Kuma et al. (1996) found no evidence for this species and instead suggested the dominance of $Fe(OH)_2^+$ and $Fe(OH)_4^-$ in this pH range. Recent studies on the solubility of iron in seawater (Byrne et al., 2000; Sunda and Huntsman, 2003) and in NaCl solution (Liu and Millero, 1999), however, suggest that the neutral species $Fe(OH)_{3(aq)}^0$ should not be ignored but assigned a lower hydrolysis constant than indicated by earlier studies.

In this study, we examine the kinetics of Fe(III) precipitation over the pH range 6.0–9.5 using a chemical definition of dissolved inorganic Fe(III) based on its accessibility to the fungal siderophore desferrioxamine B (DFB). This method avoids the possible problems (Wells et al., 1995) associated with measurement of an "operationally defined fraction" based on physical separation of the dissolved and solid forms using either 0.05 μm (Byrne and Kester, 1976a,b) or 0.02 μm (Millero et al., 1995; Kuma et al., 1996; Millero, 1998; Liu and Millero, 1999; Liu and Millero, 2002) filters. By examining competition between hydrolysis and ferrioxamine complex formation, we determine the ratio of the precipitation rate constant (k_f) and the ferrioxamine formation rate constant (k_1) in a manner similar to that used by Rose and Waite (2003). The removal of labile Fe(III) over time due to precipitation and complexation by DFB (at much lower concentrations) is also measured using ^{55}Fe radiometry and ion-pair solvent extraction of the chelated iron species (Hudson et al., 1992) and values of k_1 and then k_f subsequently determined. Variation in the precipitation rate constant with pH is then used to examine the role of the dissolved neutral species $Fe(OH)_{3(aq)}^0$ in Fe(III) precipitation.

2. Hypothesis and methods

2.1. Definitions

Labile Fe(III) (Fe′) is defined here as Fe(III) that is readily accessible to the fungal siderophore desferrioxamine B. Such labile iron should include only monomeric dissolved inorganic species [Fe^{3+}, $Fe(OH)^{2+}$, $Fe(OH)_2^+$, $Fe(OH)_{3(aq)}^0$, $Fe(OH)_4^-$ and $Fe(CO_3)_2^-$] as these will be the only forms of Fe(III) capable of rapidly forming the 1:1 Fe(III)–DFB complex. The term ferrioxamine B refers to the 1:1 Fe(III) complex with DFB, whereas desferrioxamine B refers to the free trihydroxamic acid. The term amorphous ferric oxyhydroxide (AFO) is used to refer to ferric oxyhydroxide polymers or solid phases formed in the process of precipitation.

We define precipitation as the process of losing labile Fe(III) from solution and that includes any or all of the following processes: formation of small precursor polymers (nucleation), growth of these polymers to colloidal particles (crystal growth) and subsequent condensation to a settable precipitate (ripening) (Grundl and Delwiche, 1993).

2.2. Precipitation mechanism

When Fe(III) is added to a solution, it rapidly hydrolyzes to form different ferric species. These processes are considered to exist at equilibrium at all times compared to the timescale of the other processes occurring in our system. At oversaturated concentrations, these hydrolyzed species interact with one another, initiating the precipitation process. In the presence of a strong complexing agent such as DFB, we hypothesize the occurrence of a series of competing reactions

$$Fe' + DFB \rightarrow FeDFB, \quad k_1 \tag{1}$$

$$Fe' + Fe' \rightarrow AFO_1 + nH^+, \quad k_{f1} \tag{2}$$

$$Fe' + AFO_1 \rightarrow AFO_2 + nH^+, \quad k_{f2} \tag{3a}$$

$$\dots$$

$$Fe' + AFO_{i-1} \rightarrow AFO_i + nH^+, \quad k_{fi} \tag{3b}$$

$$\dots$$

$$AFO_l + AFO_m \rightarrow AFO_{l+m} + nH^+, \quad k_{f(l+m)} \tag{4}$$

where Eq. (2) represents homogeneous nucleation, Eqs. (3a) and (3b) represent a series of reactions accounting for polymer growth by addition of monomeric Fe′ to existing polymeric AFO_i (when i is small), and Eq. (4) represents a series of reactions in which existing polymers combine to form larger polymers. In terms of the processes described earlier for loss of labile Fe(III) from solution, this reaction scheme accounts for nucleation (Eqs. (2), (3a) and (3b) when i is small), polymer growth to colloidal particles (Eqs. (3a) and (3b) when i is large and Eq. (4) when l and m are small), and aggregation to a settleable precipitate (Eq. (4) when l and/or m are large). We also account for Fe(III)

complexation to form ferrioxamine when DFB is present (Eq. (1)).

For the first set of experiments in which we aimed to determine the ratio k_f/k_1, DFB was in considerable excess of iron, i.e. $[DFB] = [DFB]_T - [FeDFB] \approx [DFB]_T$ (where the subscript T denotes the total concentration). Under these experimental conditions, we can assume that reactions like those shown in Eq. (3b) do not occur to a significant extent when i is large, as the concentration of such highly polymerized species will be relatively low over the short timescale considered. We can additionally ignore reactions of the type shown in Eq. (4), since it is only the immediate fate of Fe′ that is of concern in these experiments. Thus, the system can be described by Eqs. (1), (2), (3a), (3b). Furthermore, we hypothesize that the rate constants for homogeneous precipitation and for heterogeneous precipitation involving only small oligomers are the same, i.e. that $k_{f1} = k_i$ (when i is small). The justification for this approach is examined in the discussion of results. In this case, we can combine Eqs. (2), (3a) and (3b) to give an apparent overall precipitation reaction

$$Fe' + Fe_I \rightarrow AFO + nH^+, \quad k_f \tag{5}$$

where Fe_I is the sum of all dissolved and precipitated species (total inorganic Fe(III)).

The rate laws for ferrioxamine and AFO concentrations from Eqs. (1) and (5) are given by:

$$\frac{d[FeDFB]}{dt} = k_1[Fe'][DFB] \tag{6}$$

$$\frac{d[AFO]}{dt} = k_f[Fe'][Fe_I] \tag{7}$$

Given that $[Fe]_T = [Fe'] + [AFO] + [FeDFB]$, these rate laws may be written as

$$\frac{d[FeDFB]}{dt} = k_1[DFB]_T\{[Fe]_T - [FeDFB] - [AFO]\} \tag{8}$$

$$\frac{d[AFO]}{dt} = k_f[Fe_I]\{[Fe]_T - [FeDFB] - [AFO]\} \tag{9}$$

Solving Eqs. (8) and (9) (see electronic annex EA-1 for details) and letting $t \rightarrow \infty$ yields the equation

$$\frac{[Fe]_T}{[FeDFB]_{ss}} = \frac{k_f}{k_1} \times \frac{2[Fe]_T - [FeDFB]_{ss}}{2[DFB]_T} + 1 \tag{10}$$

where the subscript ss denotes steady-state.

Thus, a plot of $\{[Fe]_T/[FeDFB]_{ss}\}$ vs $\{(2[Fe]_T - [FeDFB]_{ss})/2[DFB]_T\}$ should be a straight line with the slope $\frac{k_f}{k_1}$ and y-intercept of 1.

For the second set of experiments in the presence of relatively low concentrations of Fe(III) and DFB, we can obtain an approximate analytical solution for k_1 by assuming that the reaction in Eq. (1) is dominant, i.e. that precipitation is negligible. This is only valid when the precipitation rate is relatively slow compared to complexation kinetics, i.e., when $k_1[Fe'][DFB] \gg k_f[Fe'][Fe_I]$. Although this approximation is quite crude when the precipitation rate is fast, it should be noted that the approximate values of k_1 obtained are used only for starting values and are subsequently refined using numerical techniques. Under this assumption we obtain the rate law:

$$\frac{d[Fe']}{dt} = -k_1[Fe'][DFB] \tag{11}$$

Since $[Fe'] = [Fe]_T - [FeDFB]$ and $[DFB] = [DFB]_T - [FeDFB]$

$$\frac{d[Fe]}{dt} = -k_1[Fe]\{[DFB]_T - [Fe]_T + [Fe]\} \tag{12}$$

Rearranging the above equation and integrating both sides gives:

$$\int \frac{d[Fe]}{[Fe]\{[DFB]_T - [Fe]_T + [Fe]\}} = -\int k_1 dt \tag{13}$$

The solution to this equation is:

$$\ln\left\{\frac{[Fe]_t}{[Fe]_T}\right\} - \ln\left\{\frac{[DFB]_T - [Fe]_T + [Fe]_t}{[DFB]_T}\right\} = -k_1\{[DFB]_T - [Fe]_T\}t \tag{14}$$

Hence a plot of $\ln\{[Fe]_t/[Fe]_T\} - \ln\{([DFB]_T - [Fe]_T + [Fe]_t)/[DFB]_T\}$ vs $-\{[DFB]_T - [Fe]_T\}t$ should be a straight line with slope k_1 (see electronic annex EA-2).

2.3. Experimental conditions

All solutions were prepared using 18 MΩ cm Milli-Q water. Chemicals were purchased from Sigma–Aldrich (unless otherwise stated). All glassware was acid washed 5 days before use. Stock solutions were refrigerated (at 4 °C) in the dark when not in use.

Solutions at various pH (6.0, 6.5, 7.0, 7.5, 8.0, 8.5 and 9.5) were prepared by adding appropriate concentrations of HCl and NaOH (Fluka puriss p.a plus) to bicarbonate solutions containing 2 mM $NaHCO_3$ and 0.01 M NaCl. Conventional organic buffers (MES and HEPES) were not used because they were found to cause interference with the absorbance measurements used for ferrioxamine determination. All pH measurements were made using a Hanna HI9025 pH meter combined with a glass electrode and Ag/AgCl reference. For measurement of pH 6.0 and 6.5, the electrode was calibrated at 25 °C using pH 4.01 and pH 7.01 buffers provided by Hanna Instruments. For measurements of pH 7.0, 7.5, 8.0, 8.5 and 9.5, the electrode was calibrated at 25 °C using Hanna Instruments pH 7.01 and pH 10.01 buffers. All buffer solutions were checked using a pH meter that had been calibrated using NIST buffer solutions. During the course of experiments (less than 5 min), no shift in pH was detectable to within ± 0.02 pH units at pH 6.0, 6.5 and 9.5. Variations of up to ± 0.05 pH were apparent at pH 7.0, 7.5, 8.0 and 8.5. Temperature was maintained at 25 ± 0.6 °C all times using a waterbath and experiments were conducted in minimum light conditions.

2.4. Determination of k_f/k_1

A stock solution of 0.5 mM Fe(III) in 2 mM HCl was prepared by dissolving 48.2 mg of reagent grade ferric ammonium sulfate dodecahydrate ($FeNH_4(SO_4)_2{\cdot}12H_2O$) (Ajax Chemicals, reagent grade) in 200 mL of HCl. A working 0.1 mM Fe(III) stock in 2 mM HCl was prepared daily by dilution of this 0.5 mM Fe(III) stock. Stock solutions of 1.0 and 10 mM DFB were prepared in Milli-Q water and were adjusted to the desired pH with addition of concentrated NaOH immediately before use.

Fe(III) was added to bicarbonate buffered solutions containing DFB and the resulting concentration of Fe(III)–DFB complex was measured colorimetrically employing a range of DFB concentrations. DFB was chosen as a complexing agent because it forms a strong complex with Fe(III) at circumneutral pH with $\log K^{\text{concd}}_{\text{Fe}^{\text{III}}\text{DFB}} = 12.1 \pm 0.6\ \text{M}^{-1}$ reported at the pH of seawater (Witter et al., 2000). In addition, DFB reacts rapidly and selectively with Fe(III) with a rate constant $k_{\text{FeDFB}} = 2 \times 10^6\ \text{M}^{-1}\ \text{s}^{-1}$ at pH 8.1 (Hudson et al., 1992; Witter et al., 2000), which is comparable with the predicted rate constant for Fe(III) precipitation (Rose and Waite, 2003). The Fe(III)–DFB complex is an orange color with a maximum absorbance at 429 nm and $\epsilon_{429} = 2280\ \text{M}^{-1}\ \text{cm}^{-1}$ at pH 8.1 (Rose and Waite, 2003) allowing spectrophotometric determination of the complex. Within the pH range examined in this study (pH 6.0–9.5), the ferrioxamine complex is recognized to possess 1:1 stoichiometry (Monzyk and Crumbliss, 1982; Farkas et al., 1999).

To determine the ratio k_f/k_1, an appropriate volume of DFB stock solution was added to 5 mL of bicarbonate-buffered solution to create DFB concentrations ranging from 4 to 100 μM. The solution pH was then adjusted by addition of HCl or NaOH immediately before addition of Fe(III). A relatively low concentration of 0.5 μM Fe(III) was used in order to minimize the effect on pH of rapid precipitation during the initial time period. Solutions were stirred vigorously at a fixed speed during the addition of HCl or NaOH and then Fe(III) stock to achieve homogeneous concentrations throughout the solution.

A peristaltic pump operating at 15 rpm was used to draw the solution through a 1.0 m path length cell (LWCC Type II, World Precision Instruments) and the absorbance of the complex formed was measured using an Ocean Optics spectrophotometry system. The spectrophotometry system consisted of light supplied by a combination of a broadband Tungsten Halogen lamp and a narrow bandwidth LED with peak light emission at 470 nm coupled with a S2000 spectrometer. To minimize interferences from external sources in the lower wavelength range, the ferrioxamine concentration was measured based on absorbance at 450 nm instead of 429 nm (with a negligible change in molar absorptivity). The absorbance at 450 nm was baseline corrected at a reference wavelength of 690 nm.

Calibration curves (linear) for ferrioxamine concentrations were developed based on the absorbance signal measured at excess DFB concentrations (100 μM DFB for pH 6.0, 6.5, 7.0, 7.5 and 9.5, and 400 μM DFB for pH 8.0 and 8.5) with high r^2 values (>0.98).

2.5. Prediction of k_1 and modeling method

^{55}Fe-radiolabeled ferric chloride in HCl solution was obtained from Perkin-Elmer. Stock solutions of 50 nM ^{55}Fe were prepared daily by diluting appropriate amounts of ^{55}Fe stock in 2 mM HCl. Stock solutions of 250 nM DFB and 10 mM HQS (8-hydroquinoline-5-sulfonate, Ajax Chemicals) were prepared in Milli-Q water. Extracting reagent stock was prepared by mixing the ion-paring reagent triotylmethylammonium chloride (Aliquot 336, Sigma–Aldrich) in toluene at a concentration of 18 g/L.

Kinetics of Fe(III) removal by complexation with DFB and by precipitation were determined using a modified version of the method described by Hudson et al. (1992). Solutions containing known concentrations of DFB were mixed with 50 nM ^{55}Fe stock in the ratio 0.5 nM ^{55}Fe:2 nM DFB and 0.5 nM ^{55}Fe:5 nM DFB and reaction time was recorded with a stopwatch. In each subsequent period of time (every 1 min for the solution containing 5 nM DFB and every 2 min for the solution containing 2 nM DFB), 4 mL of solution was pipetted into a centrifuge tube which already contained 100 μL of HQS and the mix was shaken vigorously. Rapid complexation by HQS prevents Fe(III) from being further hydrolyzed and precipitated or complexed by DFB. To extract the HQS–^{55}Fe complex, 4 mL of extracting reagent stock was added to the centrifuge tube to selectively extract the amphiphilic iron complex (HQS–^{55}Fe) and to separate it from ferrioxamine. The mixed solution was shaken continuously for 2 min allowing complete extraction. Samples were then centrifuged (at 3500 rpm) for 30 min to eliminate emulsification and the two layers subsequently separated carefully by decantation. The activity of the organic layer (upper layer), which contained the HQS–^{55}Fe, was then determined by liquid scintillation counting and calibrated to determine the concentration of labile Fe(III) complexed by HQS.

HQS was chosen to complex labile Fe(III) because it has a high stability constant for Fe(III), $\log K = 38$ (Sturgeon et al., 1981), and low affinity for major cations (Vanderborght and Van Grieken, 1977). The complex formed is easily extracted using the ion-paring reagent with high extraction efficiency (97% reported in Hudson et al. (1992) and 99% found in this study).

Modeling of results to determine k_f and k_1 was undertaken numerically using the program ACUCHEM (Braun et al., 1988) in a MATLAB interface.

3. Results and discussion

3.1. Determination of the ratio k_f/k_1

The results of 0.5 μM Fe(III) additions to bicarbonate-buffered solutions containing different initial concentra-

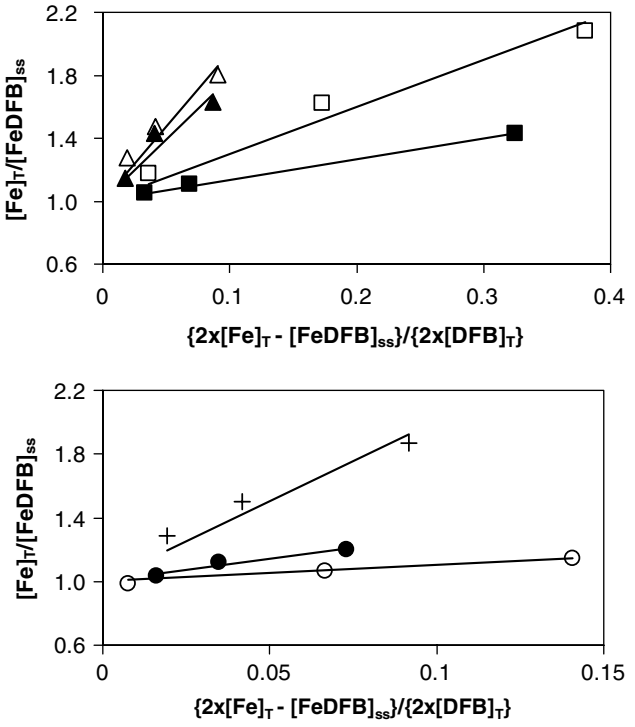

Fig. 1. Linearized data for determination of k_f/k_1 over a pH range 6.0–9.5. (■) pH 6.0, (□) pH 6.5, (▲) pH 7.0, (△) pH 7.5, (+) pH 8.0, (●) pH 8.5 and (○) pH 9.5. The solid line is of best fit with linear regression; the intercept is fixed to 1.

Table 1
Calculated values of k_f/k_1 from linear regression over a pH range 6.0–9.5

pH	6.0	6.5	7.0	7.5	8.0	8.5	9.5
Slope, k_f/k_1	1.33	2.99	7.87	9.61	10.2	3.08	1.02
r^2	1.0	0.95	0.87	0.75	0.85	0.86	0.97

tions of DFB at various pH were linearized according to Eq. (10), as shown in Fig. 1. A summary of the slopes (k_f/k_1) and the r^2 values for the linear regressions obtained are given in Table 1.

In general, the r^2 values are above 0.85 (except that at pH 7.5) indicating a good agreement between our chemical model and the observed data. The slopes (k_f/k_1) indicate that the rate of Fe(III) precipitation is generally faster than the rate of ferrioxamine formation across a wide range of examined pH (Table 1). The maximum (approximately 10-fold) difference between k_f and k_1 is observed at pH around 8.0.

3.2. Determination of k_1 and k_f

To allow us to determine actual values of k_1 and k_f in addition to their ratio, we conducted additional experiments at lower concentrations of iron and DFB at which we could observe complexation kinetics directly. For an initial estimate of k_1 values, the results of Fe(III) removal in the systems initially containing 0.5 nM ^{55}Fe and 2 nM DFB or 0.5 nM ^{55}Fe and 5 nM DFB were linearized according to Eq. (14). Results from selected pH values are shown in Fig. 2.

To refine our values for k_1 and to calculate k_f, we applied a numerical model based on the reactions shown in Eqs. (1), (2), (3a), (3b), using the initial estimates of k_1 from linearization and the previously determined ratio k_f/k_1 as starting values to fit the radiometric data obtained at different pH. The results of the model fitting process are shown in Fig. 3. A summary of k_f and k_1 values from linearization (with the r^2 values) and from the model are given in Table 2.

The values for the ferrioxamine formation rate constant fall in a narrow range with a maximum value (over the pH range examined) at pH 8.0 of $(1.6 \pm 0.15) \times 10^6\ M^{-1}\ s^{-1}$. This value is similar to the ferrioxamine formation rate constants reported by Hudson et al. (1992) and by Witter et al. (2000) in seawater of $2.0 \times 10^6\ M^{-1}\ s^{-1}$ and $2.0 \pm 1.0 \times 10^6\ M^{-1}\ s^{-1}$, respectively.

The small variations between k_1 values estimated from linearization at different initial concentrations of DFB indicate good consistency in our data. Values of k_1 determined from our analytical approximation were similar to those determined from the numerical model, except at pH 8.0, where the rate constant for precipitation is greatest. This indicates that our assumption that complexation by DFB is dominant over precipitation in the experimental system is good except around pH 8, when the effect of precipitation is significant.

In contrast with the ferrioxamine formation rate constant, which varies by only 7-fold over the experimental pH range, the precipitation rate constant varies by up to 50-fold. This latter rate constant has a maximum at pH 8.0 of $(1.6 \pm 0.15) \times 10^7\ M^{-1}\ s^{-1}$. This value is less than the value of $4.1 \times 10^7\ M^{-1}\ s^{-1}$ in seawater (pH 8.1) reported by Rose and Waite (2003). In seawater, it is likely that numerous colloids and particles that are present, even in filtered seawater (Wells et al., 1995), could act as nuclei for polymerization which enhances the process of Fe(III) precipitation. Precipitation of Fe(III) in seawater therefore may be faster than that in bicarbonate medium.

3.3. Variation in k_1 and k_f with pH

Variation of the ferrioxamine formation rate constant (k_1) with pH can be accounted for by considering both the (pH dependent) charges of the reacting species and the water loss rate (k_{-w}) of the reacting metal species (Eigen and Wilkins, 1965; Morel and Hering, 1993). The rate of water loss, which is often rate-limiting, can be significantly accelerated by metal hydrolysis, particularly in the case of slow reacting metals such as Fe(III) (Crumbliss and Garrison, 1988). At lower pH where $Fe(OH)_2^+$ is predominant (Fig. 4), the complex formation kinetics are slower than is the case at higher pH due to the slow water loss rate of this species ($k_{-w} = 10^6\ M^{-1}\ s^{-1}$) (Blesa and Matijevic, 1989). At higher pH (pH around 8.0), when

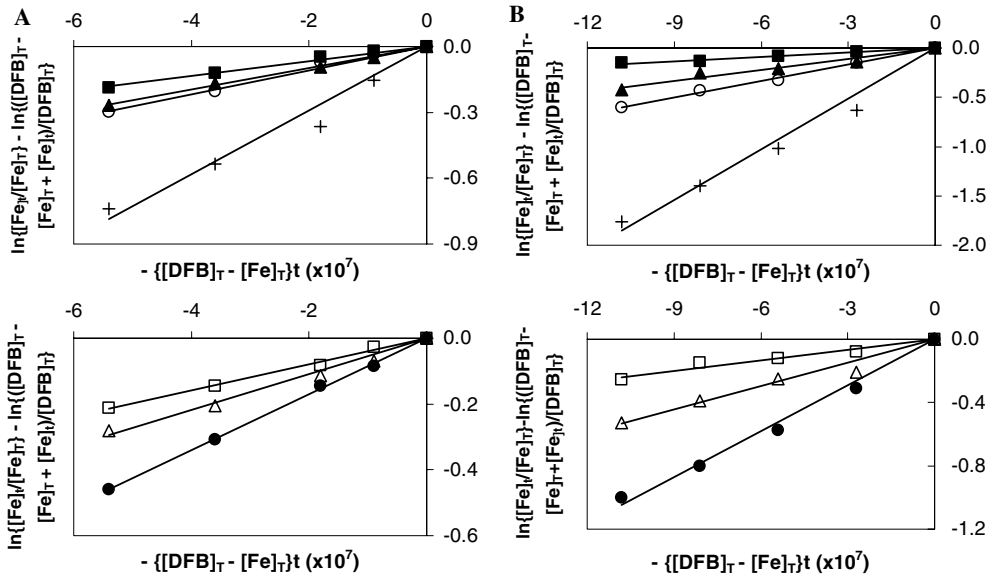

Fig. 2. Linearized data for the prediction of k_1 values over a pH range 6.0–9.5. (■) pH 6.0, (□) pH 6.5, (▲) pH 7.0, (△) pH 7.5, (+) pH 8.0, (●) pH 8.5 and (○) pH 9.5 with initial 0.5 nM ^{55}Fe and (A) with 2 nM DFB and (B) with 5 nM DFB. Solid lines are of best fit with linear regression (through the origin).

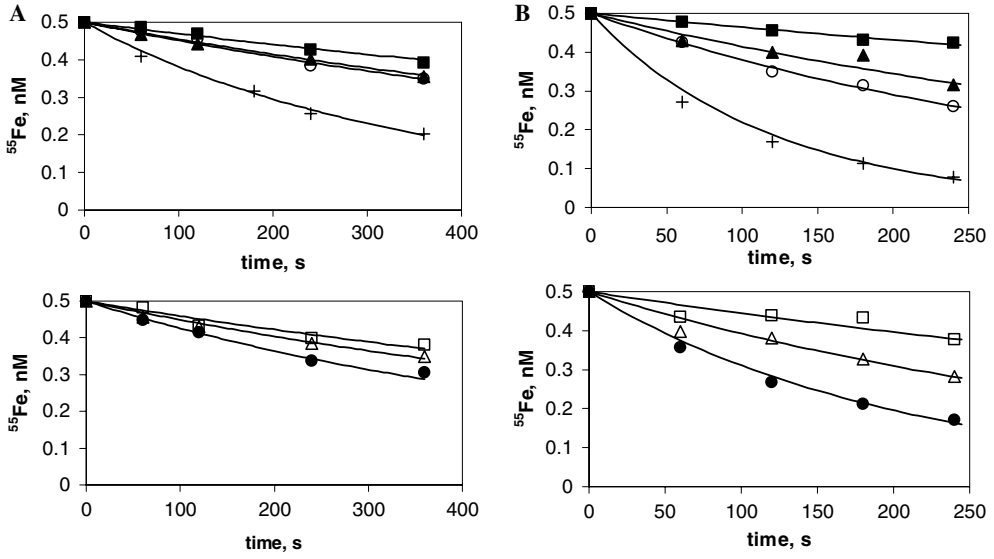

Fig. 3. Model fits and experimental data over a pH range 6.0–9.5. (■) pH 6.0, (□) pH 6.5, (▲) pH 7.0, (△) pH 7.5, (+) pH 8.0, (●) pH 8.5 and (○) pH 9.5 with initial 0.5 nM ^{55}Fe and (A) with 2 nM DFB, and (B) with 5 nM DFB.

$Fe(OH)_3{}^0$ becomes significant, the kinetics of ferrioxamine formation is faster. This is expected because $Fe(OH)_3{}^0$ may have a higher water loss rate than $Fe(OH)_2{}^+$, presumably similar to a small oligomer for which $k_{-w} = 2.6 \times 10^7$ $M^{-1}\,s^{-1}$ (Blesa and Matijevic, 1989). When $Fe(OH)_4{}^-$ becomes dominant at high pH (pH > 8.5), the effect of the negative charge of the reacting species ($Fe(OH)_4{}^-$ and the deprotonated ligand) may significantly decrease the ferrioxamine formation rate, even though the water loss rate of $Fe(OH)_4{}^-$ is predicted to be high (Schneider, 1988). Note that the pKs for deprotonation of desferriferrioxamine B are 8.3, 9.0, 9.6 and 10.8 at $I = 0.1$ and 25 °C (Evers et al., 1989) and thus the ligand progressively deprotonates at pH values above 8.3. Therefore, the decrease in k_1 at pH values above 8 is consistent with an electrostatic repulsion effect.

In contrast to the small variation in k_1, k_f varied by nearly two orders of magnitude across the pH range considered. Interestingly, the variation of k_f was seen to vary in a manner that was similar to the variation in concentration of $Fe(OH)_{3(aq)}{}^0$ (Fig. 4). Stability constants used to calculate the concentrations of different ferric species with pH in 2 mM $NaHCO_3$ and 0.01 M NaCl are given in Table 3. (A detailed justification of the stability constants used is given in Electronic Annex EA-3.)

This observation suggests that the dominant mechanism for iron precipitation in the pH range considered involves

Table 2
Calculated values of k_1 from linear regression and modeled values of k_1 and k_f over a pH range 6.0–9.5

pH	Estimated k_1 ($\times 10^6$ M^{-1} s^{-1})[a,b]	r^{2b}	Modeled k_1 ($\times 10^6$ M^{-1} s^{-1})[b]	Modeled k_f ($\times 10^6$ M^{-1} s^{-1})[b]	Estimated k_1 ($\times 10^6$ M^{-1} s^{-1})[a,c]	r^{2c}	Modeled k_1 ($\times 10^6$ M^{-1} s^{-1})[c]	Modeled k_f ($\times 10^6$ M^{-1} s^{-1})[c]	Modeled k_1 ($\times 10^6$ M^{-1} s^{-1})[d]	Modeled k_f ($\times 10^6$ M^{-1} s^{-1})[d]
6.0	0.34	0.97	0.32	0.43	0.15	0.98	0.15	0.20	0.24 ± 0.09	0.32 ± 0.12
6.5	0.43	1.00	0.43	1.29	0.22	0.91	0.24	0.70	0.34 ± 0.10	1.0 ± 0.30
7.0	0.49	0.98	0.48	3.78	0.36	0.96	0.38	3.0	0.43 ± 0.05	3.4 ± 0.39
7.5	0.55	0.99	0.55	5.24	0.49	0.98	0.49	4.7	0.52 ± 0.03	5.0 ± 0.27
8.0	1.0	0.99	1.4	14	1.00	0.98	1.7	17	1.6 ± 0.15	16 ± 1.5
8.5	0.85	1.00	0.82	2.53	0.97	0.99	0.97	3.0	0.90 ± 0.08	2.8 ± 0.24
9.5	0.52	0.98	0.52	0.53	0.56	0.99	0.56	0.57	0.54 ± 0.02	0.55 ± 0.02

[a] Determined by linearization method.
[b] 0.5 nM ^{55}Fe:2 nM DFB.
[c] 0.5 nM ^{55}Fe:5 nM DFB.
[d] Average values.

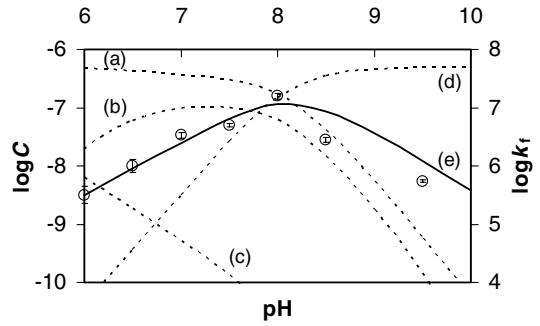

Fig. 4. Log C vs pH of various important Fe(III) species at pH 6.0–9.5 in 0.01 M NaCl and 2 mM $NaHCO_3$, $[Fe(III)]_T = 0.5$ μM. Fe(III) species of concentration less than 10^{-10} M including chloride complexes and sulfate complexes are not shown. Data were computed using MINEQL+. Symbols: (a) $Fe(OH)_2^+$, (b) $Fe(CO_3)_2^-$, (c) $Fe(OH)^{2+}$, (d) $Fe(OH)_4^-$, (e) $Fe(OH)_{3(aq)}^0$ and (Θ) log(k_f), k_f is the precipitation rate constant, M^{-1} s^{-1}.

Table 3
Hydrolysis and overall formation constants for Fe(III) complexes in pure water at 25 °C used in Fe(III) speciation model (β, mol kg^{-1} H_2O)

Species	log β^a
$Fe(OH)^{2+}$	$-2.13^{b,c}$
$Fe(OH)_2^+$	$-6.13^{b,c}$
$Fe(OH)_{3(aq)}^0$	$-14.3^{b,d}$
$Fe(OH)_4^-$	$-22.2^{b,e}$
$FeCl^{2+}$	$1.28^{f,g}$
$FeCl_2^+$	$1.16^{f,g}$
$Fe(SO_4)^+$	$4.27^{f,g}$
$Fe(SO_4)_2^-$	$6.11^{f,g}$
$Fe(CO_3)_2^-$	$19.6^{f,h}$

Further discussion of these constants is given in Electronic Annex EA-3
[a] Davies equation used for ionic strength correction.
[b] Hydrolysis constants $\beta_i = \frac{[Fe(OH)_i^{3-i}][H^+]^i}{[Fe^{3+}]}$.
[c] Byrne et al. (2000).
[d] This study.
[e] Liu and Millero (1999).
[f] $\beta_{FeL_i^{3-ni}} = \frac{[FeL_i^{3-ni}]}{[Fe^{3+}][L^{n-}]^i}$.
[g] Millero et al. (1995).
[h] Bruno and Duro (2000).

$Fe(OH)_{3(aq)}^0$ as a precursor species, as previously suggested by Melikhov et al. (1987) and Grundl and Delwiche (1993). If we consider the mechanism proposed for iron precipitation under our experimental conditions in Eq. (5), rewriting in terms of a reaction between the neutral species and any other iron species (together denoted as Fe_I) gives the reaction

$$Fe_I + Fe(OH)_{3(aq)}^0 \rightarrow AFO, k_{Fe(OH)_3^0} \quad (15)$$

The rate of disappearance of dissolved iron due to this reaction is then given by

$$-\frac{d[Fe']}{dt} = k_{Fe(OH)_3^0}[Fe(OH)_{3(aq)}^0][Fe_I] = k_f[Fe'][Fe_I] \quad (16)$$

Dividing Eq. (16) by $[Fe_I]$ gives

$$k_f = k_{Fe(OH)_3^0}\alpha_{Fe(OH)_3^0} \quad (17)$$

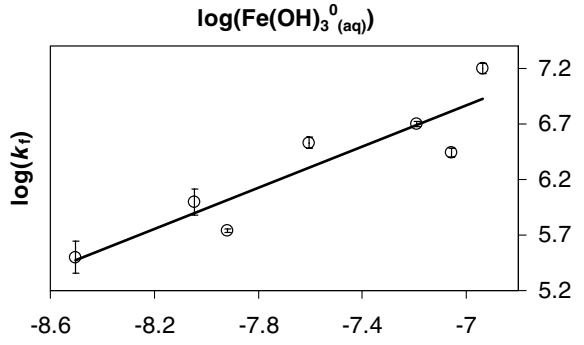

Fig. 5. Relationship between concentration of neutral ferric species, $Fe(OH)_{3(aq)}^{0}$ and rate constant of Fe(III) precipitation over a pH range 6.0–9.5. Error bars are standard error from measurements at initial 2 and 5 nM DFB concentrations.

Table 4
Rate constants for water exchange at 25 °C

Species	k_{-w} (s^{-1})
Fe^{3+}	1.67×10^{2}[a]
$Fe(OH)^{2+}$	4.5×10^{5}[a]
$Fe(OH)_2^{+}$	1.0×10^{6}[a]
$Fe(OH)_3^{0}$	6.3×10^{7}[b]
$Fe(OH)_4^{-}$	$< 1.0 \times 10^{6}$[b]
$Fe(CO_3)_2^{-}$	$<1.0 \times 10^{6}$[b]

[a] Blesa and Matijevic (1989).
[b] Determined in this work assuming that water loss is rate limiting (note that this is unlikely to be the case for the $Fe(OH)_4^{-}$ species).

$$\text{i.e.,}\quad \log(k_f) = \log(k_{Fe(OH)_3^0}\alpha_{Fe(OH)_3^0}) = \log\left(\frac{k_{Fe(OH)_3^0}}{[Fe]_T}\right) + \log[Fe(OH)_{3(aq)}^{0}] \qquad (18)$$

where $\alpha_{Fe(OH)_3^0}$ is the fraction of $Fe(OH)_{3(aq)}^{0}$ in the total dissolved inorganic iron pool.

Thus, plotting $\log(k_f)$ vs $\log[Fe(OH)_{3(aq)}^{0}]$ should result in a slope of 1 and y-intercept of $\log\left(\frac{k_{Fe(OH)_3^0}}{[Fe]_T}\right)$, as shown in Fig. 5. The experimental data plotted in Fig. 5 is consistent with the model (Eq. (18)) based on the hypothetical chemical reaction (Eq. (15)) and yields a slope of 0.97, $r^2 = 0.88$ and y-intercept of 13.6. Hence, the value of the intrinsic rate constant for the precipitation of $Fe(OH)_{3(aq)}^{0}$ is calculated to be $k_{Fe(OH)_3^0} = 2.0 \times 10^{7} M^{-1} s^{-1}$. This value is considerably less than the rate constant for diffusion-controlled reaction of two identical neutral species of $\sim 7.9 \times 10^{9}\ M^{-1}\ s^{-1}$ (Morel and Hering, 1993), suggesting that diffusion is not the rate-limiting step in the polymerization reaction. Examination of the sensitivity of the observed correspondence between $\log(k_f)$ and $\log[Fe(OH)_{3(aq)}^{0}]$ by varying the formation constants over a range of possible values shows little impact of the choice of formation constant for $Fe(CO_3)_2^{-}$ (or, indeed, whether it is present or absent). Changing the value of $\log \beta_3^0$ over the range -14.3 to -14.1 (and maintaining the other constants as shown in Table 4) did not change the direct dependence of $\log(k_f)$ on $\log[Fe(OH)_{3(aq)}^{0}]$ but did alter the estimated value of $k_{Fe(OH)_3^0}$. The intrinsic rate constant for the precipitation of $Fe(OH)_{3(aq)}^{0}$, $k_{Fe(OH)_3^0}$ also varied significantly (from 9.1×10^{6} to $9.1 \times 10^{7}\ M^{-1}\ s^{-1}$) for changes in $\log \beta_2^0$ and $\log \beta_4^0$ over possible ranges but the direct dependence of $\log(k_f)$ on $\log[Fe(OH)_{3(aq)}^{0}]$ was reasonably maintained with slopes ranging from 0.85 to 1.1.

One explanation for the observed direct dependence between $\log(k_f)$ and $\log[Fe(OH)_{3(aq)}^{0}]$ is that the rate-limiting step in the process is loss of coordinated water from the encounter complex that initially results from the collision of dissolved monomeric iron. This idea has been proposed previously (Eigen and Wilkins, 1965; Schneider, 1988; Blesa and Matijevic, 1989) in analogy to the Eigen–Wilkins mechanism for complex formation. As it is typically loss of the first water molecule that is the rate-limiting step, we would expect the rate constant for the reaction of the neutrally charged $Fe(OH)_{3(aq)}^{0}$ species with any other iron species to be about $10^{-0.5}$ times the rate of water loss from $Fe(OH)_{3(aq)}^{0}$ (Morel and Hering, 1993). Hence the determined value of $k_{Fe(OH)_3^0} = 2.0 \times 10^{7} M^{-1} s^{-1}$ would correspond to a water exchange rate constant of $6.3 \times 10^{7}\ s^{-1}$. This is in reasonable agreement with the value of $2.6 \times 10^{7}\ s^{-1}$ reported for a small iron oxyhydroxide oligomer by Blesa and Matijevic (1989), which would be expected to exhibit a similar rate of water exchange due to its similar charge per iron atom.

Such polymerization reactions are not limited to the neutral $Fe(OH)_{3(aq)}^{0}$ species. Formation of dimers in acidic solutions at high iron concentrations is known to occur (with further polymerization ultimately resulting in formation of a precipitate) and iron precipitation at pH above 12 is believed to occur via reaction of $Fe(OH)_4^{-}$ (Schneider, 1988). However reactions between the charged hydrolysis species are quite slow at low pH, due to a combination of electrostatic repulsion and decreasing rates of water exchange with lesser degrees of hydrolysis (Morel and Hering, 1993). To simulate this generalized mechanism across a range of pH, we predicted the rate constant k_f as a function of pH by considering the potential reactions of all hydrolyzed iron species with all other hydrolyzed iron species at each pH. The rate constant for the polymerization reaction was calculated as the product of the stability constant for the encounter complex, K_{os}, and the rate constant for water exchange, k_{-w}. Values for K_{os} vary according to the sum of the charges of the reacting species and were taken from Morel and Hering (1993), whereas values for k_{-w} were used as shown in Table 4. The overall rate constant was then calculated as $k_f = \sum_i \sum_j k_{ij}\alpha_i\alpha_j$, where k_{ij} is the rate constant for reaction between species i and species j, and α_i is the fraction of species i at a particular pH calculated from the stability constants in Table 3.

The predicted value of the rate constant k_f is shown in Fig. 6 across a wide range of pH values, along with the experimental data. In the process of calculating k_f, it was necessary to estimate the value of k_{-w} for the species

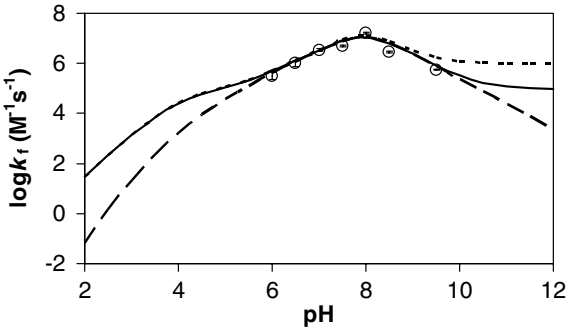

Fig. 6. Experimental and predicted k_f values across a wide range of pH. (Θ) experimental data, (- -) all Fe(III) hydrolyzed species with k_{-w} ($Fe(OH)_4^-$) = $1.0 \times 10^7\ s^{-1}$, (—) all Fe(III) hydrolyzed species with k_{-w} ($Fe(OH)_4^-$) = $1.0 \times 10^6\ s^{-1}$, (– –) only $Fe(OH)_{3(aq)}^0$ species.

$Fe(OH)_4^-$, as its value has not been determined experimentally. It is clear from Fig. 6 that if the kinetics of iron polymerization are governed by the rate of water loss, the value of k_{-w} for the species $Fe(OH)_4^-$ must be no more than $1.0 \times 10^6\ s^{-1}$, otherwise the predicted values of k_f greatly exceed the measured values at the higher pHs. Previously, this rate constant has been estimated as $\sim 10^9\ s^{-1}$ (Morel and Hering, 1993) based on observations that an increase in the degree of hydrolysis generally results in an increase in the rate of water exchange. Thus, a k_{-w} of $1.0 \times 10^6\ s^{-1}$ or less for $Fe(OH)_4^-$ is clearly at odds with this estimate and suggests that, for the negatively charged Fe(III) hydroxide complex, a process other than water loss is rate limiting. At the higher pH values, the growth of iron hydroxide polymers involves a reaction between $Fe(OH)_4^-$ and other $[Fe(OH)_3]_n$ polymers, which will be negatively charged at high pH due to increasing hydrolysis. Thus the two species will repel one another. For the polymerization reaction to occur, once a water is lost from the coordination sphere of $Fe(OH)_4^-$, it must be replaced by a coordinated water or hydroxide from the coordination sphere of one of the iron atoms in the negatively charged ferric polymer. The increasing hydrolysis and resulting negative charge of the polymers as pH is raised should greatly slow the reaction rate. Thus, the reaction rate will be approximated by the water exchange rate so long as the rate limiting step is the loss of water from the coordination sphere of the complex. However, at high levels of hydrolysis (e.g., for $Fe(OH)_4^-$), the water loss rates are fast, and the subsequent re-coordination rates are slowed due to electrostatic repulsion. Consequently, under these circumstances, the latter re-coordination reaction is expected to be the rate limiting step.

Two other features in Fig. 6 deserve attention. First, the predicted values of k_f are in reasonable agreement with the measured values of k_f across a wide range of experimental pH. This agreement validates our selection of formation rate constants of different Fe(III) species. Second, although polymerization reactions between hydrolysis species other than $Fe(OH)_{3(aq)}^0$ clearly have a significant impact on the predicted values of k_f at high and low pH values, ignoring these reactions has only a small effect on the predicted value of k_f in the pH range over which k_f was experimentally determined. Indeed, the predicted and measured values of k_f correlate very strongly with $r^2 = 0.76$ and slope = 1.1. Thus, it is clear that the kinetics of water loss in the polymerization of $Fe(OH)_{3(aq)}^0$ can account for the observed values of k_f, and that polymerization of $Fe(OH)_{3(aq)}^0$, rather than other hydrolysis species, dominates in the pH range 6.0–9.5.

3.4. Modelling approach and model alternatives

According to Stumm and Morgan (1996), there are various processes involved in the formation of a solid phase from an oversaturated solution of which three steps are often distinguished, as described below:

1. The interaction between Fe(III) species leads to the formation of critical clusters or nuclei:

$$Fe' + Fe' \iff X_1$$
$$Fe' + X_1 \iff X_2$$
$$\cdots$$
$$Fe' + X_{j-1} \iff X_j \text{ (critical cluster)}$$
$$Fe' + X_j \iff X_{j+1} \text{ (nucleation)}$$

2. Subsequently, material is deposited on these nuclei and crystallites are formed:

$$Fe' + X_{j+1} \rightarrow AFO \rightarrow AFO \text{ (crystal growth)}$$

3. Large crystals are formed from fine amorphous crystallites:

$$AFO + AFO \rightarrow \text{Crystallites (ripening)}$$

Under the reaction conditions in this study, excess concentrations of DFB lead to the completion of reactions in milliseconds, with the majority of Fe(III) ending up in the complexed form. The experimental signal observed in this short time period is likely to represent the reaction processes in step 1 and possibly in the early stages of step 2. In this situation, the rate of removal of dissolved Fe(III) from solution thus exhibits a first-order dependence on the concentration of total inorganic Fe(III) (dissolved ferric species and small polymers).

It could be argued that only the dissolved ferric species participate in reactions under these experimental conditions, i.e. that the reaction shown in Eqs. (3a) and (3b) does not occur at all. It is also possible to derive an analytical solution to such a system and, by use of a Taylor series expansion, to linearize the experimental data to obtain the ratio k_f/k_1. In this case, the ratios obtained at the different pH values show a similar pH dependence, but are about 45% larger than those obtained using the approach presented earlier. Therefore in both types of approach, the data support the involvement of the neutral dissolved

$Fe(OH)_{3(aq)}^{0}$ as the major initiator of precipitation reactions, and support the likelihood that such reactions are governed by water loss kinetics. Based on this mechanism, we would expect reaction between $Fe(OH)_{3(aq)}^{0}$ and any other iron species (dissolved or polymeric) to proceed at an equal rate, since there is no charge effect as long as one of the reacting species is neutral $Fe(OH)_{3(aq)}^{0}$ in this case, and the rate-limiting loss of the first water molecule will always occur from the $Fe(OH)_{3(aq)}^{0}$ molecule, given its fast water exchange kinetics. Therefore, the approach used in this work, in which we consider dissolved iron to precipitate by reaction with either dissolved or small polymeric species at an equal rate, appears to be correct.

It is important to note, however, that the values of k_f determined using this approach will only apply when all iron atoms in a polymer can potentially react with a $Fe(OH)_{3(aq)}^{0}$ molecule. When precipitation is dominated by the second stage described above, in which crystalline growth is occurring, many iron atoms will be inaccessible to dissolved iron, and thus the apparent rate of precipitation (with regard to the total inorganic iron concentration) would be expected to decrease.

3.5. Validity of experimental approach

Limitations of our experimental technique may exist, specifically regarding the mixing process (ferric stock with DFB) and extraction of the sulfoxine-organic layer in the presence of ferrioxamine. Poor mixing on the rapid timescale of the reactions investigated may result in heterogeneity to occur locally. Furthermore, careless extraction may lead to misinterpretation of the results. However, the fact that we did not see high inter-replicate variability or systematic variation among treatments suggests that such experimental errors were not important in this work.

It is also possible in the second set of experiments that within the 30 min time period during extraction before the two layers were separated, newly formed ferric polymers may have dissolved and been complexed by sulfoxine, leading to an erroneously high measurement of free iron. We would expect this error to be negligible because the concentration of precipitated iron is insignificant, except perhaps at pH 8.0. At this pH, we would expect that up to ~35% of amorphous ferric oxyhydroxide may re-dissolve into the sulfoxine-labile pool within 30 min (Rose and Waite, 2003) which may slightly influence the calculated values of k_1 and k_f at this pH. However, based on the estimated amount of iron that could potentially re-dissolve, we would not expect the error associated with the value of k_f at pH 8.0 to be significantly greater than that already reported from replicate analysis (relative standard error ~10%).

4. Conclusions and implications

In this study, we have successfully modeled and calculated the rate of Fe(III) precipitation in synthetic bicarbonate solutions. Over a range of examined pH (6.0–9.5), the kinetics of complexation of Fe(III) by the fungal siderophore desferrioxamine B is slower than the kinetics of precipitation, but similarly exhibits a maximum rate constant at about pH 8. This indicates that natural organic ligands, when present in sufficient concentrations, may successfully compete with precipitation for available Fe(III) to maintain an extremely low concentration of dissolved inorganic Fe(III) in the water column.

The study also supports the existence of the neutral Fe(III) species $Fe(OH)_{3(aq)}^{0}$ due to the apparently dominant role it plays in the precipitation process around neutral pH. The relationship between the rate constant for precipitation and the concentration of $Fe(OH)_{3(aq)}^{0}$ has been firmly established, allowing us to predict rates of Fe(III) precipitation between pH 6.0 and 9.5. It appears that the kinetics of Fe(III) precipitation may be governed by water exchange kinetics during the polymerization process. As $Fe(OH)_{3(aq)}^{0}$ rapidly exchanges bound water molecules, it would be expected to polymerize much more rapidly than positively charged dissolved ferric hydrolysis species. Furthermore, the fact that this species is uncharged and will likely control the rate-limiting water loss step during polymerization reactions suggests that it will react equally fast with any dissolved or polymeric iron species present in the water column. While it has not been measured, the rate of water loss from $Fe(OH)_4^-$ is expected to be fast. In this case, the re-coordination between $Fe(OH)_4^-$ and negatively charged Fe(III) polymers following water loss is expected to be rate limiting as a result of electrostatic repulsion effects.

While the results of this study provide for prediction of the rate of Fe(III) precipitation over a range of pH in synthetic bicarbonate solutions, more work is needed to describe the complete process of precipitation in nature. In natural waters, it is likely that numerous particles of different sizes are present, encouraging the process of precipitation to occur heterogeneously. The process of crystal growth and ripening therefore may also be particularly important in the precipitation process in natural waters.

Acknowledgments

We gratefully acknowledge the scholarship support provided to A. Ninh Pham by the CRC for Water Quality and Treatment and the advice provided by Drs. Peter Hawkins of Sydney Water Corporation and Bala Vigneswaran of the Sydney Catchment Authority. We also thank Robert H. Byrne, William Sunda and other anonymous reviewers for their very helpful comments on an earlier version of the manuscript.

Associate editor: Robert H. Byrne

Appendix A. Supplementary data

Supplementary data associated with this article can be found, in the online version, at doi:10.1016/j.gca.2005.10.018.

References

Baes, C.F., Mesmer, R.E., 1976. *The Hydrolysis of Cations*. A Wiley-Interscience Publication.

Blesa, M.A., Matijevic, E., 1989. Phase transformations of iron oxides, oxohydroxides, and hydrous oxides in aqueous media. *Adv. Colloid Interface Sci.* **29**, 173–221.

Braun, W., Herron, J.T., Kahaner, D.K., 1988. ACUCHEM: a computer program for modeling complex chemical reaction systems. *Intl. J. Chem. Kinet.* **20**, 51–62.

Bruno, J., Duro, L., 2000. Reply to W. Hummel's comment on and correction to ''On the influence of carbonate in mineral dissolution: I. The thermodynamics and kinetics of hematite dissolution in bicarbonate solution at T = 25 °C by J. Bruno, W. Stumm, P. Wersin and F. Brandberg. *Geochim. Cosmochim. Acta* **64**(12), 2173–2176.

Byrne, R.H., Kester, D.R., 1976a. Solubility of hydrous ferric oxide and iron speciation in seawater. *Mar. Chem.* **4**, 255–274.

Byrne, R.H., Kester, D.R., 1976b. A potentiometric study of ferric ion complexes in synthetic media and seawater. *Mar. Chem.* **4**, 275–287.

Byrne, R.H., Luo, Y.-R., Young, R.W., 2000. Iron hydrolysis and solubility revisited: observations and comments on iron hydrolysis characterizations. *Mar. Chem.* **70**, 23–35.

Byrne, R.H., Luo, Y.-R., 2000. Direct observation of nonintegral hydrous ferric oxide solubility products: $K_{SO}^{*} = [Fe^{3+}][H^{+}]^{-2.86}$. *Geochim. Cosmochim. Acta* **64**, 1873–1877.

Crumbliss, A.L., Garrison, J.M., 1988. A comparison of some aspects of the aqueous coordination chemistry of aluminum(III) and iron(III). *Comments Inorg. Chem.* **8**, 1–26.

Eigen, M., Wilkins, R.G., 1965. Kinetics and mechanisms of formation of metal complexes. In: Marmann, R.K., Fraser, R.T., Bouman (Eds.), Mechanisms of Inorganic Reactions. *J. Adv. Chem. Ser.* **49**, pp. 55–80.

Evers, A., Hancock, R.D., Martell, A.E., Motekaitis, R.J., 1989. Metal-ion recognition in ligands with negatively charged oxygen donor groups—complexation of Fe(III), Ga(III), In(III), Al(III), and other highly charged metal-ions. *Inorg. Chem.* **28** (11), 2189–2195.

Farkas, E., Enyedy, E.A., Csoka, H., 1999. A comparison between the chelating properties of some dihydroxamic acids, desferrioxamine B and acetohydroxamic acid. *Polyhedron* **18**, 2391–2398.

Flynn, C.M., 1984. Hydrolysis of inorganic iron(III) salts. *Chem. Rev.* **84**, 31–41.

Grundl, T., Delwiche, J., 1993. Kinetics of ferric oxyhydroxide precipitation. *J. Contam. Hydrol.* **14**, 71–97.

Hudson, R.J.M., Covault, D.T., Morel, F.M.M., 1992. Investigations of iron coordination and redox reactions in seawater using ^{59}Fe radiometry and ion-pair solvent extraction of amphiphilic iron complexes. *Mar. Chem.* **38**, 209–235.

Kuma, K., Nakabayashi, S., Suzuki, Y., Matsunaga, K., 1992. Dissolution rate and solubility of colloidal hydrous ferric oxide in seawater. *Mar. Chem.* **38**, 133–143.

Kuma, K., Nishioka, J., Matsunaga, K., 1996. Controls on iron(III) hydroxide solubility in seawater: the influence of pH and natural organic chelators. *Limnol. Oceanogr.* **41** (3), 396–407.

Liu, X., Millero, F.J., 1999. The solubility of iron hydroxide in sodium chloride solutions. *Geochim. Cosmochim. Acta* **63**, 3487–3497.

Liu, X., Millero, F.J., 2002. The solubility of iron in seawater. *Mar. Chem.* **77**, 43–54.

Melikhov, I.V., Kozlovskaya, E.D., Berliner, L.B., Prokofiev, M.A., 1987. Kinetics of hydroxide Fe(III) solid phase formation. *J. Colloid Interface Sci.* **117** (1), 1–9.

Millero, F.J., Yao, W., Aicher, J., 1995. The speciation of Fe(II) and Fe(III) in natural waters. *Mar. Chem.* **50**, 21–39.

Millero, F.J., 1998. Solubility of Fe(III) in seawater. *Earth Planet. Sci. Lett.* **154**, 323–329.

Monzyk, B., Crumbliss, A.L., 1982. Kinetics and mechanism of the stepwise dissociation of Iron(III) from ferrioxamine B in aqueous acid. *J. Am. Chem. Soc.* **104**, 4921–4929.

Morel, F.M.M., Hering, J.G., 1993. *Principles and Applications of Aquatic Chemistry*. John Wiley & Sons, Inc, A Wiley-Interscience Publication.

Perera, W.N., Hefter, G., 2003. Mononuclear cyano- and hydroxo-complexes of Iron(III). *Inorg. Chem.* **42**, 5917–5923.

Rose, A.L., Waite, T.D., 2003. Kinetics of hydrolysis and precipitation of ferric iron in seawater. *Environ. Sci. Technol.* **37**, 3897–3903.

Schneider, W., 1988. Iron hydrolysis and the biochemistry of iron-the interplay of hydroxide and biogenic ligands. *Chimia* **42**, 9–20.

Stumm, W., Morgan, J.J., 1996. *Aquatic Chemistry: Chemical Equilibria and Rates in Natural Waters*. John Wiley and Sons, Inc.

Sturgeon, R.E., Berman, S.S., Willie, S.N., Desaulniers, J.A.H., 1981. Preconcentration of trace elements from seawater with silica-immobilized 8-hydroxyquinoline. *Anal. Chem.* **53**, 2337–2340.

Sunda, W., Huntsman, S., 2003. Effect of pH, light, and temperature on Fe-EDTA chelation and Fe hydrolysis in seawater. *Mar. Chem.* **84**, 35–47.

Vanderborght, B.M., Van Grieken, R.E., 1977. Enrichment of trace metals in water by adsorption on activated carbon. *Anal. Chem.* **49**, 311–316.

Waite, T.D., 2001. Themodynamics of the iron system in seawater. In: Turner, D.R., Hunter, K.A. (Eds.), *Biogeochemistry of Iron in Seawater*. Wiley, West Sussex, England, pp. 291–342.

Wells, M.L., Price, N.M., Bruland, K.K., 1995. Iron chemistry in seawater and its relationship to phytoplankton: a workshop report. *Mar. Chem.* **48**, 157–182.

Witter, A.E., Hutchins, D.A., Butler, A., Luther III, G.W., 2000. Determination of conditional stability constants and kinetic constants for strong model Fe-binding ligands in seawater. *Mar. Chem.* **69**, 1–17.

Zafiriou, O.C., True, M.B., 1980. Interconversion of iron(III) hydroxy complexes in seawater. *Mar. Chem.* **8**, 281–288.